Network-Side Mobile Position Location Using Factor Graphs

Jung-Chieh Chen, Yeong-Cheng Wang, Ching-Shyang Maa, and Jiunn-Tsair Chen

***Abstract*— A low-complexity high-accuracy algorithm is proposed to estimate the location of a target MS based on network-side time-of-arrival (TOA) measurements. Under a factor graph framework, the proposed algorithm first constructs a graphical model for the mobile position location problem by dividing the problem into many mutually-interactive local constraints. Each local constraint is enforced by a separate local processing unit. Efficient exchange of soft-information among local processing units in the mobile switching center (MSC) then iteratively purifies the estimate of the MS location. Numerical results show that the proposed algorithm not only enjoys low complexity, suitable for integrated-circuit implementation, but it is also able to achieve performance very close to the optimum achievable solution accuracy, the maximum likelihood (ML) solution accuracy.**

***Index Terms*— TOA, position location, factor graph, soft-information.**

I. Introduction

POSITIONING mobile locations in wireless communication systems is crucial to many applications, such as the US Enhanced-911 (E-911), location-sensitive billing, fraud detection, and so on. Position location (PL) methods for cellular systems can be divided into two categories: handset-side and network-side methods. In the handset-side methods, multiple base stations (BSs) emit signals toward the target mobile station (MS). The target MS then utilizes the received signals to estimate its location through triangulation techniques. In the network-side methods, signals are transmitted from the target MS to its neighboring BSs. The MS location is thus collectively determined by the BSs. For safety consideration, the US Federal Communications Commission (FCC) requires the wireless communication service providers to obtain the location information of any MS in the service area with such accuracy as to allow only 1) 50 m of maximum error tolerance in 67 percent of scenarios and 150 m of that in 95 percent of scenarios for handset-side methods and 2) 100 m of maximum error tolerance in 67 percent of scenarios and 300 m of that in 95 percent of scenarios for network-side methods [1]. In addition, wireless geolocation technology is considered a key enabling technology [2], because it has great potential to promote many other related applications that could significantly expand the wireless user base. Thus, the investigation into accurately estimating the location of an MS has drawn more and more attention from cellular and personal communication service providers. Several third generation (3G) wireless communication systems such as IMT/UMTS [2] have been among the first to adopt location strategies in their standards.

Wireless geolocation techniques of locating an MS in a wireless communication system make use of measurements on signal strength, time-of-arrival (TOA), angle-of-arrival (AOA), or their combinations [3]-[6]. Each technique has its own advantages and limitations. For example, the TOA PL schemes require at least three properly-located BSs to estimate a two-dimensional (2-D) MS location, and they generally achieve better accuracy than the AOA PL schemes. The AOA PL schemes, on the other hand, require as few as two BSs for a location estimate. However, the AOA PL schemes are highly range dependent. A small error in the angle measurement will result in a large location error if the target MS is far away from any involved BS.

In general, it is up to the system designer to decide whether to adopt the handset-side method or the network-side method. However, a position location calculator must be included into each handset for the handset-side method, while no modification is required in the handset for the network-side method. It should be noted that the IMT/UMTS [2] proposals for the 3G systems do not impose much (if any) extra implementation complexity in positioning the mobile location on the MS side. Thus, this paper is interested only in the network-side PL problems. On the other hand, the channelization schemes proposed for the 3G cellular networks, such as wideband code-division multiple access (WCDMA) systems, make the TOA PL scheme very attractive because the high chip rates in the WCDMA systems allow for high accuracy in TOA measurement. At the same time, several recently-published papers [7], [8] have been drawing attention to methods of location in time-division multiple access (TDMA) systems, especially GSM systems. In a TDMA system, each BS is required to maintain time-slot synchronization among the received signals from all the associated MSs. The TOA PL scheme is thus a convenient choice in TDMA systems to support a location system. This paper, therefore, concentrates on the TOA PL schemes applied to the network side.

In the TOA PL schemes, each TOA measurement made at a BS produces a circle, centered at the BS. The target MS is supposed to locate at somewhere on the circle. If all TOA measurements are exclusively related to line-of-sight[2] (LOS)

Manuscript received August 10, 2003; revised February 19, 2004, June 11, 2004, and January 5, 2005; accepted January 27, 2005. The associate editor coordinating the review of this letter and approving it for publication was J. K. Tugnait.

J.-C. Chen is with Department of Optoelectronics and Communication Engineering, National Kaohsiung Normal University, Kaohsiung 802, Taiwan, R.O.C. (e-mail: jcchen@nknucc.nknu.edu.tw).

C.-S. Maa and J.-T. Chen are with the Institute of Communications Engineering, National Tsing Hua University, Hsinchu 30055, Taiwan, R.O.C. (e-mail: d899603@alumni.nthu.edu.tw, jtchen@ee.nthu.edu.tw).

Y.-C.Wang is with the Department of Information Management, VaNung University, 1 Van-Nung Road, Chung-Li 32061, Taiwan, R.O.C. (e-mail: starwang@msa.vnu.edu.tw).

Digital Object Identifier 10.1109/TWC.2006.03401.

signals and assume no TOA measurement error, making use of at least three circles produced by TOA measurements at three different BSs, one can identify the 2-D MS location as the intersection of these circles. Due to the nonlinearity of the circular lines of position (LOP), one can only formulate the PL problem by a set of nonlinear equations, which are difficult to solve directly.

A traditional way to solve the PL problem is to calculate the least square (LS) solution after applying the Taylor series linearization (TS-LS) [9]. The TS-LS algorithm can provide reasonably accurate location estimates, but it requires an initial location guess and may suffer from the convergence problem if the initial guess is not good enough. Alternatively, Caffery [8] proposed a simple geometrical approach in which straight linear LOPs, rather than circular LOPs, are used to determine the location of the MS. The basic idea of the geometrical algorithm is to reduce a set of second-order LOP equations with two unknowns into a set of first-order LOP linear equations with the same two unknowns, so as to reduce the algorithm complexity. However, the accuracy of the geometrical algorithm is always lower than that of the TS-LS algorithm given a good initial location guess.

In [10], we proposed a low-complexity high-accuracy novel iterative PL algorithm, which takes into consideration the stochastic properties of the range measurement errors. To effectively utilize the available stochastic information, based on a factor graph [11] framework, soft-information is created and exchanged among local processing units in the proposed algorithm to obtain the location estimates of the target MS. In this paper, we elaborate the proposed PL algorithm and correct a mishandling of the range measurement data[3] in [10]. In addition, we provide analytic and further simulation results, which show that the proposed algorithm not only enjoys low complexity, easy to implement, but it is also able to perform very close to the optimum achievable PL accuracy, the maximum likelihood (ML) solution accuracy.

This paper is organized as follows. In Section 2, we describe a PL system model. Next, the proposed PL algorithm is developed in Section 3. Some performance bounds of the PL problem are derived in Section 4. Simulation results that compare the performance bounds and the estimation errors of various location algorithms, including the proposed one, are given in Section 5.

II. System Model

In a network-side PL system, TOA measurement can be conducted in one of the following two manners: 1) Uplink measurement: The TOAs of the signals from the target MS are measured by at least three different BSs. This requires accurate time reference between the MS and all the involved BSs. It should be noted that an incorrect TOA-clock timing-offset of just 1 μs will introduce a position error of 300 meters. 2) Round-trip measurement: The round-trip time of signals transmitted from the BSs are measured. While at least three BSs broadcast signals toward the target MS, the target MS responds to each of the three BSs by re-transmitting the received signals immediately. The PL system then utilizes half of each round-trip time to estimate the distance from the corresponding BS to the MS and to calculate the location of the MS. No time reference is needed in the round-trip measurement. In the Universal Terrestrial Radio Access Network (UTRAN), the Round Trip Time (RTT) is introduced as a system parameter [1].

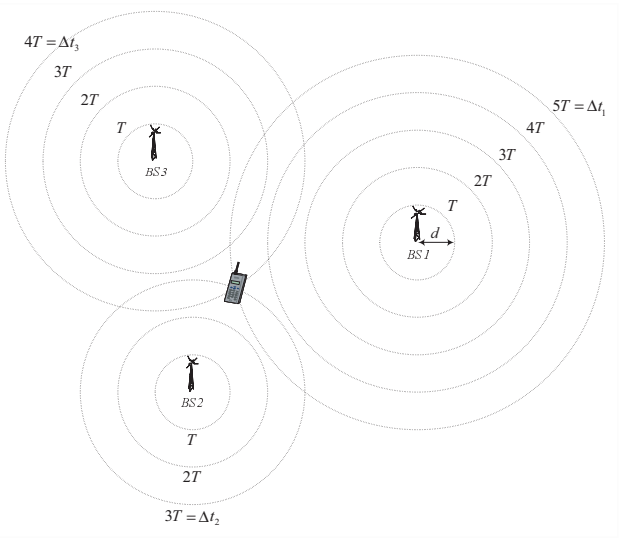

Fig. 1. An example of TOA measurement, where $T = \frac{d}{c}$ and c is the speed of light.

With the knowledge that the electromagnetic waves propagate at the speed of light, we have

$$\widehat{d}_i = c \cdot \Delta t_i;\ i = 1, 2, \cdots, N, \tag{1}$$

where c is the speed of light, Δt_i is the measurement of one-way TOA difference between the target MS and the i^{th} BS, $\widehat{d}_i$ is the associated range measurement of a true range value d_i, and N is the total number of the involved BSs. As an example in Fig. 1, a radio wave is emitted from each of $N = 3$ BSs. The TOA differences from the target MS to the three BSs, *BS 1*, *BS 2*, and *BS 3*, are Δt_1, Δt_2 and Δt_3, respectively. Therefore, the MS is expected to be $\widehat{d}_1 = c \cdot \Delta t_1$ distance away from *BS 1*. Similar rules can be applied to *BS 2* and *BS 3*. The location of the MS in the two dimensional service area can then be determined as follows: As mentioned in Section 1, each TOA measurement produces a circle. We thus plot N circles, each of which has the location of one BS as its center and the corresponding range measurement as its radius. If there is neither measurement error nor non-line-of-sight (NLOS) error, the N circles would intersect at exactly one point, which is the location of the target MS. The relation between the unknown MS location and the known BS locations is given by

$$\widehat{d}_i = f_i(x, y) = \sqrt{(x - X_i)^2 + (y - Y_i)^2}; i = 1, 2, \ldots, N, \tag{2}$$

where (x, y) is the unknown coordinate vector of the MS, and

[2]It should be noted that another factor that inhibits accurate PL is the measurement errors caused by the non-line-of-sight (NLOS) paths between the MS and the BS. However, in this paper, we focus on coping with the noise-induced measurement errors.

[3]The information of measurement error should enter the factor graph through range measurement nodes, $\{D_i\}$ in Fig. 3, not through nodes handling translations between x and $\{\Delta x_i\}$ (or between y and $\{\Delta y_i\}$) as did in [10].

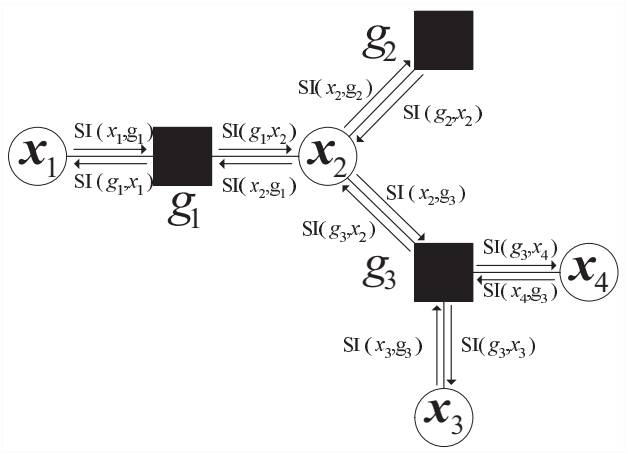

Fig. 2. A simple factor graph representation of $g(x_1, x_2, x_3, x_4) = g_1(x_1, x_2) \cdot g_2(x_2) \cdot g_3(x_2, x_3, x_4)$ with agent nodes g_1, g_2, g_3 and variable nodes x_1, x_2, x_3, x_4.

(X_i, Y_i) is the known coordinate vector of the i^{th} BS. Given $\{\Delta t_i\}$ as the available measurement data in (1), the problem in question now is to solve (2) to obtain the MS location (x, y).

However, TOA measurement errors do occur. Due to accumulated effect of many independent factors, the TOA measurement errors can be reasonably modeled as Gaussian random variables, as also done in [12], [13]. The stochastic properties of these random variables will be used in this paper to develop a novel TOA PL algorithm and derive some performance bounds.

III. The Algorithm

Equation (2) defines a set of N nonlinear equations, $\{f_i(x, y); i = 1, 2, \ldots, N\}$, whose solution is the location of the target MS. In such a 2-D setting, it is a complex problem. In this section, we first reduce the 2-D problem to two 1-D problem and then use a factor graph to efficiently process all the measurement data to obtain a near-optimum MS location estimate. In the following subsections, we first briefly summarize the idea of factor graph [11], and then describe the PL system in terms of a factor graph model. Next, with the help of the factor graph, a new algorithm for MS position location is proposed.

A. Factor Graph and Sum-Product Algorithm

To set the notation straight, we first start with the description of a generic factor graph. A factor graph is a bipartite graph that illustrates how a complicated *global* function (*global* task) of many variables factors into the product of several simple *local* functions (*local* tasks), each of which is a function of very few variables. A factor graph consists of two kinds of nodes: variable nodes and agent (function) nodes. An edge connects a variable node x and an agent node g_i, named after its associated local function $g_i(\cdot)$, if and only if x is an argument of $g_i(\cdot)$. Shown in Fig. 2 is a simple factor graph representation of $g(x_1, x_2, x_3, x_4) = g_1(x_1, x_2) \cdot g_2(x_2) \cdot g_3(x_2, x_3, x_4)$ with agent nodes g_1, g_2, g_3 and variable nodes x_1, x_2, x_3, x_4. The solution of variables to a problem described by a factor graph is usually obtained through an iterative soft-information-passing procedure among variable nodes and agent nodes based on the sum-product algorithm [11], to be briefly summarized next.

A piece of soft-information, describing the stochastic properties of an associated variable, passed from a variable node to an agent node is simply the product of all the soft-information coming from the other neighboring agent nodes to the variable node. For example, as shown in Fig. 2, the soft-information passed from x_2 to g_3 is given by

$$\mathrm{SI}(x_2, g_3) = \mathrm{SI}(g_1, x_2) \cdot \mathrm{SI}(g_2, x_2), \tag{3}$$

where $\mathrm{SI}(a, b)$ denotes the soft-information passed from node a to node b. On the other hand, a piece of soft-information passed from an agent node to a variable node is the product of a local function associated with the agent node and all the soft-information coming from the other neighboring variable nodes to the agent node, summarized over all the related variables except the variable associated with the variable node receiving soft-information. In Fig. 2, the soft information passed from g_3 to x_2 can be expressed as

$$\mathrm{SI}(g_3, x_2) = \int_{x_3} \int_{x_4} g_3(x_2, x_3, x_4) \cdot \mathrm{SI}(x_3, g_3) \cdot \mathrm{SI}(x_4, g_3)\, dx_3\, dx_4, \tag{4}$$

where $g_3(x_2, x_3, x_4)$ is the associated local function, i.e., the constraint rule of the agent node g_3 to define the mutual relation among x_2, x_3 and x_4.

With these two rules, soft-information is iteratively passed around among neighboring nodes. After the soft-information converges, the estimation of each variable can be made based on the overall soft-information of the corresponding variable node, defined as the product of all incoming soft-information, e.g., the overall soft-information of x_2 can be written as

$$\mathrm{SI}(x_2) = \mathrm{SI}(g_1, x_2) \cdot \mathrm{SI}(g_2, x_2) \cdot \mathrm{SI}(g_3, x_2). \tag{5}$$

B. Factor Graph Model

For a TOA PL scheme, all information available at the position determination entity (PDE) includes 1) the known coordinates of the involved BSs, and 2) TOA/range measurement data and their the stochastic properties [12], especially the variances $\{\sigma_{d_i}^2\}$ of the range measurement errors in (1). In practice, the variances of the TOA/range measurement errors depend on channel bandwidth, BS antenna parameters, and wireless environments. They can be estimated based on 1) the signal-to-noise ratio (SNR) of the received signals and 2) their typical values in various wireless environments [13]. The probability density function[4] (pdf) of the TOA/range measurement can then be constructed and serve as valuable soft-information for MS position location. Consequently, the accuracy of an MS location estimate will depend on how to utilize the available soft-information effectively and sufficiently. To make the best use of the soft-information, in this section, we propose a novel algorithm under a factor graph framework, as described next.

[4]It should be noted that the proposed algorithm needs the stochastic properties of the measurement data to construct and to exchange soft-information before the location of the target MS can be estimated. However, even with much-less-than-perfect error statistics, the proposed algorithm can still provide a great help in terms of performance upgrade.

The spirit of the factor graph is to factor a function of many variables into the product of "several" functions, each is a function of very few variables. That means the original "complex" function is broken down into several "simple" ones. In other word, the original problem is broken down into several easier-to-deal-with sub-problems, to be solved jointly and iteratively. The power of the factor graph approach lies in its ability to distributively process local variables, to effortlessly solve the problem, and to frequently provide the optimum solution or close-to-optimum solutions; which make the factor graph approach a popular candidate for solving distributed problems. On the other hand, the PL problem, by its nature, is a distributed problem, i.e., parameters in the PL problem are only locally related. Therefore, it is an excellent match in introducing the factor graph approach to solve for the PL problem. Based on this spirit, the proposed factor graph model, as illustrated in Fig. 3(a), factors the original complex TOA-based PL problem into several simple local problems, each is represented by an agent node.

In order to reduce the complexity of the 2-D problem, we divide the problem into two 1-D problems based on the geometric relationship between the target MS and the involved BSs. The two 1-D problems are respectively represented by two main groups of nodes in the factor graph, $x-$coordinate group and $y-$coordinate group, as illustrated in Fig. 3(a). Each main group contains N subgroups, where N is the total number of the involved BSs. Each subgroup assigned an agent node either A_i or B_i describes both the direction and the distance of the target MS as related to the i^{th} associated BS in the referred coordinate. On the other hand, the statistics of the range measurements enter the factor graph through agent nodes $\{D_i\}$. The two main groups and the range measurement information are then merged at agent nodes $\{C_i\}$.

The signed relative distances from the MS to the i^{th} BS in the referred coordinate can be described as

$$\begin{cases} \Delta x_i = X_i - x \\ \Delta y_i = Y_i - y \end{cases} ; i = 1, 2, \cdots, N, \tag{6}$$

which are the constraint rules respectively for agent nodes A_i and B_i. The constraint rule for agent node C_i can be described by the Pythagorean law, $(\Delta x_i)^2 + (\Delta y_i)^2 = d_i^2$, where d_i is the range from the i^{th} BS to the target MS. For the purpose of maintaining low complexity, as will become clear in the next subsection, we assume Gaussian statistics for all the variables in Fig. 3(a). This assumption may not reflect the exact pdf's of all the variables perfectly, but it plays a crucial role in carrying the soft-information around within the factor graph. Under this assumption, the pdf of d_i produced by the agent node D_i is Gaussian with its mean equals the range measurement $\widehat{d}_i$ and with its variance equals the variance of the range measurement $\sigma_{d_i}^2$. For convenience, we use the notation

$$\mathcal{N}\left(x, m, \sigma^2\right) \propto \exp\left[-\frac{(x-m)^2}{2\sigma^2}\right] \tag{7}$$

to represent a Gaussian pdf, with x being a dummy variable and with m and σ^2 being the mean and variance, respectively. Hence, the soft-information $\mathrm{SI}\left(D_i, d_i\right) = \mathcal{N}\left(d_i, \widehat{d}_i, \sigma_{d_i}^2\right)$ describes the constraint rules of agent node D_i.

In the sense of the physical layout in the cellular system, the factor graph for the proposed system model in Fig. 3(a) can be reorganized into Fig. 3(b). As shown in Fig. 3(b), within the mobile switching center (MSC), the processing units with respect to the same BS are brought together. We partition the PL system into N *distributed* parts and each part includes three agent nodes and two variable nodes. Each node in Fig. 3(b) is meant to carry out only some simple calculations.

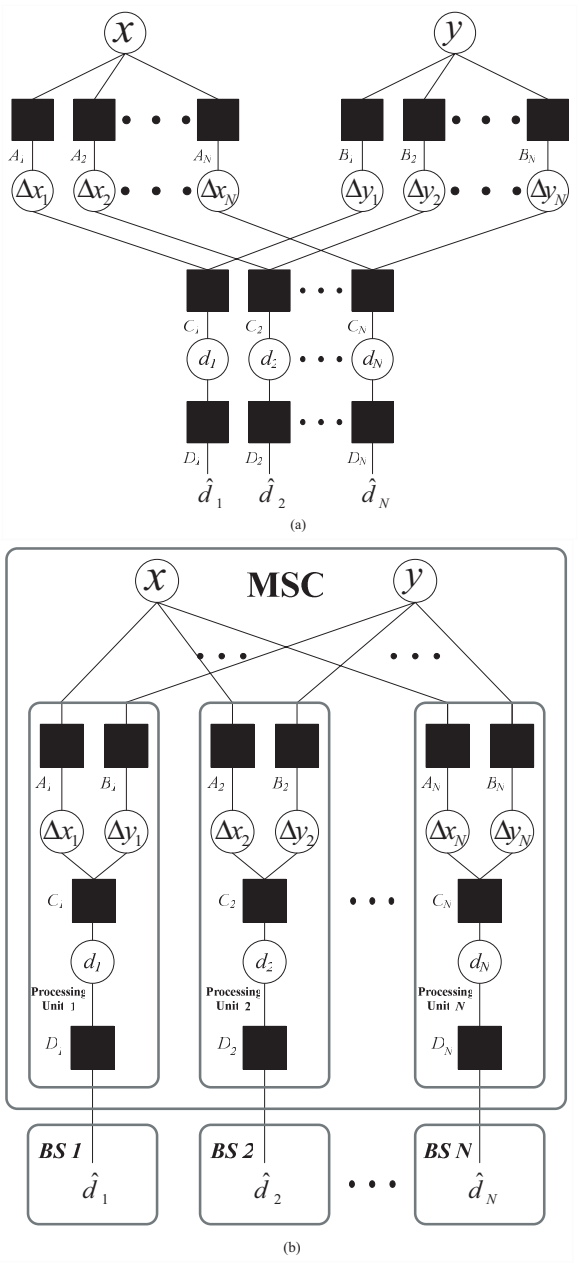

Fig. 3. Factor graph representations of the proposed TOA-based PL system in terms of (a) $x-y$ coordinates (b) physical layout.

C. Soft-Information Calculation

In this section, we describe in detail the operations conducted by each node in Fig. 3(b). At the very beginning, a rough MS location estimate $\left(x^0, y^0\right)$ is obtained by using a 3-BS geometrical algorithm [8]. At this time, except for the variables $\{d_i\}$, all the other variables carry deterministic values, the degenerated pdf of each is Gaussian with a fixed mean and with zero variance. Note that the superscript of x^0 and y^0 denotes the iteration index. Also note that the first

nodes to process the soft-information should be agent nodes $\{C_i\}$ at initialization, so as to make all the involved Gaussian pdf's have non-zero variances.

After initialization, soft-information is processed and passed around between the variable nodes and the agent nodes. We next introduce the operations carried out on the soft-information by each variable node and each agent node in Fig. 3(b) as follows:

1) Variable nodes x and y:
Based on (3), the first rule described in Section 3.1, the soft-information passed from variable node $\widehat{x}$ to agent node A_i in the k^{th} iteration is a Guassian pdf of x^k and can be expressed as

$$\mathrm{SI}\left(x^k, A_i^k\right) = \prod_{j \neq i} \mathrm{SI}\left(A_j^k, x^k\right), \tag{8}$$

where the superscript k again denotes the iteration index and $\mathrm{SI}\left(A_j^k, x^k\right)$ is a Gaussian pdf of x^k. Note that the product of any J Gaussian pdf's is also Gaussian and can be simply derived as [11]

$$\prod_{j=1}^{J} \mathcal{N}\left(x, m_j, \sigma_j^2\right) \propto \mathcal{N}\left(x, m_\Lambda, \sigma_\Lambda^2\right) \tag{9}$$

where

$$\frac{1}{\sigma_\Lambda^2} = \sum_{j=1}^{J} \frac{1}{\sigma_j^2} \tag{10}$$

and

$$m_\Lambda = \sigma_\Lambda^2 \sum_{j=1}^{J} \frac{m_j}{\sigma_j^2}. \tag{11}$$

From (9), (10) and (11), the calculation of (8) is just simple arithmetic. A similar procedure, as that described above for variable node x, can be applied to variable node y.

2) Variable nodes Δx_i, Δy_i, and d_i:
According to (3) again, variable node Δx_i directly passes the Gaussian pdf's of Δx_i,

$$\mathrm{SI}\left(\Delta x_i^k, A_i^k\right) = \mathrm{SI}\left(C_i^k, \Delta x_i^k\right) \tag{12}$$

and

$$\mathrm{SI}\left(\Delta x_i^k, C_i^k\right) = \mathrm{SI}\left(A_i^k, \Delta x_i^k\right), \tag{13}$$

as the soft-information between agent nodes A_i and C_i. It is the same for variable node Δy_i with respect to agent nodes B_i and C_i and variable node d_i with respect to agent nodes C_i and D_i.

3) Agent nodes A_i and B_i:
The functions of agent nodes A_i and B_i are to convert the relative location information into the absolute location information, and vice versa. Therefore, the soft-information passed from agent node A_i to variable node Δx_i in the k^{th} iteration is a Gaussian pdf of Δx_i^k expressed as $\mathcal{N}\left(\Delta x_i^k, X_i - m_{x^k}, \sigma_{x^k}^2\right)$, where m_{x^k} and $\sigma_{x^k}^2$ are respectively the mean and the variance of the Gaussian soft-information from variable node x^k. On the other hand, the soft-information passed from variable node A_i to agent node x in the k^{th} iteration is a Gaussian pdf of x_i^k expressed as $\mathcal{N}\left(x^k, X_i - m_{\Delta x_i^k}, \sigma_{\Delta x_i^k}^2\right)$, where $m_{\Delta x_i^k}$ and $\sigma_{\Delta x_i^k}^2$ are respectively the mean and the variance of the Gaussian soft-information from variable node Δx_i^k. Again, a similar procedure, as that described above for agent node A_i, can be applied to agent node B_i

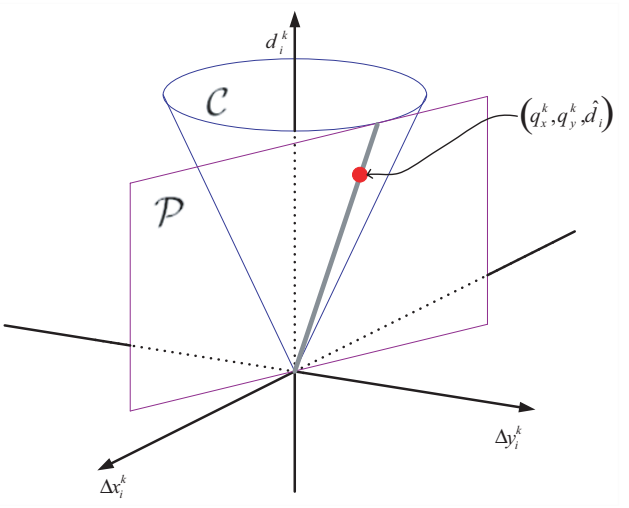

Fig. 4. Linear approximation of (14) around the local area centered at $\left(q_x^k, q_y^k, \widehat{d}_i\right)$.

4) Agent node C_i:
The agent nodes $\{C_i\}$ play an important role in converting the soft-information between the $x-$coordinate ground and the $y-$coordinate group. According to the Pythagorean law, the constraint rule between variable node Δx_i and variable node Δy_i can be described by

$$\left(d_i^k\right)^2 = \left(\Delta x_i^k\right)^2 + \left(\Delta y_i^k\right)^2, \tag{14}$$

shown as cone $\mathcal{C}$ in Fig. 4. Let us first derive the soft-information passed from agent node C_i to variable node Δy_i. In order to keep the soft-information Gaussian, some approximation has to be made: We construct a tangent plane to linearly approximate cone $\mathcal{C}$ in a local region. Let plane $\mathcal{P}$ be the tangent plane with a contact line going through both the origin and the center point of local approximation, denoted by $\left(q_x^k, q_y^k, \widehat{d}_i\right)$. The $x-$coordinate q_x^k of the center point $\left(q_x^k, q_y^k, \widehat{d}_i\right)$ is the MS relative location estimate in the $x-$coordinate, i.e., the mean value of Δx_i^k which has a Gaussian pdf, $\mathrm{SI}\left(\Delta x_i^k, C_i^k\right)$, and the $y-$coordinate $q_y^k = \pm\sqrt{\left(\widehat{d}_i\right)^2 - q_x^k}$. We thus obtain a linear constraint between Δx_i^k, Δy_i^k, and d_i to locally approximate (14). The linear equation of plane $\mathcal{P}$ can be written as

$$\Delta y_i^k = \xi \cdot \Delta x_i^k + \chi \cdot d_i^k, \tag{15}$$

where $\xi = -q_x^k / q_y^k$, and $\chi = \frac{1}{\widehat{d}_i}\left(q_y^k - \xi \cdot q_x^k\right)$. Since $\mathrm{SI}\left(\Delta x_i^k, C_i^k\right)$ and $\mathrm{SI}\left(d_i^k, C_i^k\right)$ are both Gaussian and (15) is a linear mapping, the soft-information passed from agent node C_i to variable node Δy_i is also

Gaussian and can be expressed as

$$\mathrm{SI}\left(C_i^k, \Delta y_i^{k+1}\right) = \mathcal{N}\left(\Delta y_i^{k+1}, q_y^k, \xi^2\eta_x^k + \chi^2\sigma_{d_i}^2\right), \tag{16}$$

where η_x^k is the variance of the Gaussian soft-information $\mathrm{SI}\left(\Delta x_i^k, C_i^k\right)$ and $\sigma_{d_i}^2$ is the variance of the Gaussian soft-information $\mathrm{SI}\left(d_i^k, C_i^k\right)$. Similarly, the soft-information $\mathrm{SI}\left(C_i^k, \Delta x_i^{k+1}\right)$ passed from agent node C_i to variable node Δx_i can be derived in an identical procedure described above.

In each round of iteration, according to (5), the MS location estimate can be updated by the product of the soft-information coming from all the edges connected to the variable nodes x and y, $\mathrm{SI}\left(x^k\right) = \prod_{j=1}^{N} \mathrm{SI}\left(A_j^k, x^k\right)$ and $\mathrm{SI}\left(y^k\right) = \prod_{j=1}^{N} \mathrm{SI}\left(B_j^k, y^k\right)$. After the soft-information converges, the decision on the MS location can be made as the mean value of the Gaussian distributions, $\mathrm{SI}(x^k)$ and $\mathrm{SI}(y^k)$. Note that the analysis of the convergence properties for the proposed algorithm is extremely difficult. We are still working on it and have reached no conclusive results so far. Therefore, the convergence analysis will not be covered in this paper. We can only point out that all the functions involved in the proposed algorithm seem always well behaved in terms of the convergence problem.

To highlight the low-complexity characteristics of the proposed system, the required operations for each node in the factor graph are summarized in Table I. It is clearly shown in Table I that only the means and the variances of the incoming Gaussian pdf's need to be processed to produce the mean and variance of the outgoing Gaussian pdf, and only very little calculation is needed in each node. The distributed nature of the factor graph also makes the proposed system highly suitable for integrated-circuit implementation.

TABLE I

THE OPERATIONS REQUIRED FOR THE NODES DEFINED IN FIG. 6(B).

Node	(mean,variance)	
	input	output
A_i	(m_i,σ_i^2)	$(X_i - m_i,\sigma_i^2)$
B_i	(m_i,σ_i^2)	$(Y_i - m_i,\sigma_i^2)$
C_i	$(m_i,\sigma_i^2,\widehat{d}_i,\sigma_{d_i}^2)$	$\left(\pm\sqrt{\widehat{d}_i^2 - m_i^2}, \frac{m_i^2\sigma_i^2+\widehat{d}_i^2\sigma_{d_i}^2}{\widehat{d}_i^2-m_i^2}\right)$
D_i	$(\widehat{d}_i,0)$	$(\widehat{d}_i,\sigma_{d_i}^2)$
Δx_i, Δy_i and d_i	(m_i,σ_i^2)	(m_i,σ_i^2)
x and y	$(m_j,\sigma_j^2), j \neq i$	$\left(\sigma_i^2\sum_{j\neq i}\frac{m_j}{\sigma_j^2}, \sigma_i^2 = \frac{1}{\sum_{j\neq i}\frac{1}{\sigma_j^2}}\right)$

IV. PERFORMANCE BOUNDS

For a fair comparison between the algorithm proposed in Section 3 and the existing algorithms described in [8], [9], in this section, we derive several performance bounds so as to construct a skeleton of performance criteria for each algorithm to fit in. In Section 4.1, we derive the least square bound, named LS solution accuracy in this paper, for the estimation errors of the TOA PL schemes. Next, in Sections 4.2, we derive the maximum likelihood bounds, named ML solution accuracy in this paper, assuming Gaussian pdf's for the TOA measurement errors.

A. Least Square Solution Accuracy

Let us define the least square solution accuracy as the average error of the target MS location estimate with the least square criterion. Unlike the TS-LS algorithm, the LS solution does not ignore the nonlinear higher order terms. Therefore, the LS solution accuracy is an estimation error lower bound for the TS-LS algorithm. In principle, the LS approach for a TOA-based PL problem is confined to solving

$$(\widehat{x},\widehat{y}) = \arg\min_{(x,y)\in R^2} h_{\mathrm{LS}}(x,y), \tag{17}$$

where

$$h_{\mathrm{LS}}(x,y) = \sum_{i=1}^{N}\left[\widehat{d}_i - \sqrt{(X_i-x)^2+(Y_i-y)^2}\right]^2. \tag{18}$$

The solution to (23) can be obtained by equating the partial derivatives of h_{LS}, with respect to x and y, to zero,

$$\begin{cases} \frac{\partial h_{\mathrm{LS}}}{\partial x} = \sum_{i=1}^{N}(X_i - x)\left[\frac{\widehat{d}_i}{\sqrt{(X_i-x)^2+(Y_i-y)^2}} - 1\right] = 0 \\ \frac{\partial h_{\mathrm{LS}}}{\partial y} = \sum_{i=1}^{N}(Y_i - y)\left[\frac{\widehat{d}_i}{\sqrt{(X_i-x)^2+(Y_i-y)^2}} - 1\right] = 0 \end{cases}. \tag{19}$$

The solution to (19) is the solution to a system of non-linear equations. Numerical methods can be utilized to obtain a location estimate. The sample average of the location estimation errors then provides a good approximation for the LS solution accuracy. Note that the LS approach is infeasible due to its high complexity, but the LS solution accuracy serves as an estimation error lower bound for all the PL algorithms belonging to the LS family, which covers almost all the existing PL algorithms including the TS-LS algorithm [9] and the geometrical algorithm [8].

B. ML Solution Accuracy with Gaussian TOA/Range Measurement Errors

The LS solution accuracy is not an estimation error lower bound for the proposed algorithm since no stochastic properties of the TOA/range measurement errors are considered in the LS solution. On the other hand, the ML solution accuracy, defined as the average error of the target MS location estimate with the maximum likelihood criterion, is an overall estimation error lower bound for any practical feasible algorithm if the assumed pdf's of the TOA/range measurement errors are correct. Different stochastic properties of the measurement errors result in different ML solution accuracys. In this subsection, we assume that 1) the measurement errors among different MS-BS pairs are independent, and 2) the pdf of each TOA/range measurement error with respect to the measurement data $\widehat{d}_i$ is Gaussian with variance $\sigma_{d_i}^2$. Hence, conditioning on the exact MS location, the joint likelihood function for the distance estimates $\widehat{d}_1, \widehat{d}_2, \cdots, \widehat{d}_N$ can be expressed as (20) where $\kappa = \prod_{i=1}^{N}\frac{1}{\sqrt{2\pi}\sigma_{d_i}}$ is a constant. To derive an ML solution

$$L(\widehat{d}_1, \widehat{d}_2, \cdots, \widehat{d}_N \Big| x, y) = \prod_{i=1}^{N} p_i(\widehat{d}_i \Big| x, y) \tag{20}$$

$$= \kappa \cdot \exp\left\{ -\sum_{i=1}^{N} \frac{\left[\widehat{d}_i - \sqrt{(X_i - x)^2 + (Y_i - y)^2}\right]^2}{2\sigma_{d_i}^2} \right\}. \tag{21}$$

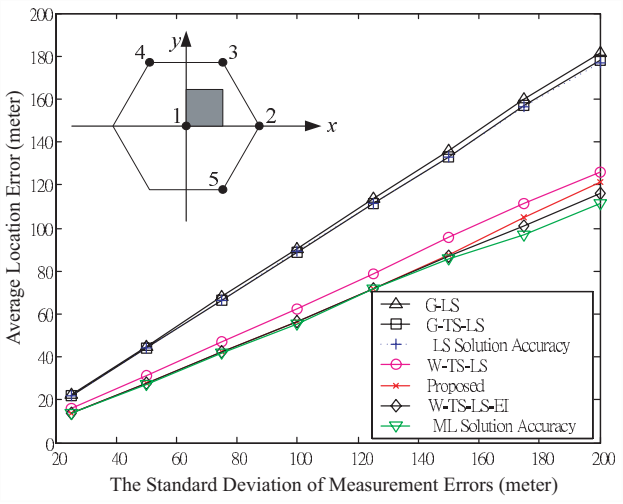

Fig. 5. Performance comparison between LS solution accuracy, ML solution accuracy, G-TS-LS, G-LS,W-TS-LS, W-TS-LS-EI, and the proposed factor graph approaches with a hexagonal cellular layout. The range measurement error model is Gaussian distribution with the standard deviation ranging from 25 to 200 meters.

to (21), we differentiate (21) with respect to x and y and equate them to zero,

$$\begin{cases} \frac{\partial L}{\partial x} = \sum_{i=1}^{N} \frac{1}{\sigma_{d_i}^2} (X_i - x) \left[\frac{\widehat{d}_i}{\sqrt{(X_i - x)^2 + (Y_i - y)^2}} - 1 \right] = 0 \\ \frac{\partial L}{\partial y} = \sum_{i=1}^{N} \frac{1}{\sigma_{d_i}^2} (Y_i - y) \left[\frac{\widehat{d}_i}{\sqrt{(X_i - x)^2 + (Y_i - y)^2}} - 1 \right] = 0 \end{cases}. \tag{22}$$

It is obvious that (22) is again a system of non-linear equations. Although the ML solution is the optimum achievable solution, solving for an ML estimate is extremely complex. However, through numerical methods, the sample average of the estimation errors for the target MS location approximates the ML solution accuracy. As will be shown in Section 5, the proposed algorithm presented in Section 3 can achieve performance very close to the ML solution accuracy, while its complexity remains low.

It should be noted that the literature in estimation theory often compare the performance of an estimation to the Cramer-Rao Lower Bound (CRLB), which is a minimum variance lower bound of an unbiased estimator. However, the CRLB is achievable only in some scenarios, where the measurement noise is zero-mean Gaussian [14]. In this paper, we adopt the ML solution accuracy as the overall lower bound because it is always achievable. The CRLB for the TOA-based PL problem can be found in [15].

V. Simulation Results

Simulations are conducted to verify the performance improvement of the PL system introduced by the proposed algorithm. For comparison, we also test three existing algorithms: 1) the geometrical LS algorithm (G-LS) [8], 2) the geometrical-algorithm-aided TS-LS algorithm (G-TS-LS) [9], which is identical to the TS-LS algorithm, except that it uses the MS location estimate obtained from the G-LS algorithm, not a random coordinate vector, as its initial guess, and 3) another algorithm modified from the G-TS-LS algorithm, named W-TS-LS, which takes into account the noise variance includes in the G-TS-LS algorithm to produce more accurate results. In order to clarify the sources of the performance differences among these algorithms, we also numerically evaluate two performance bounds, the LS solution accuracy and the optimum ML solution accuracy. The simulation scenario is exactly the same as that in [13]: We consider a standard hexagonal cellular network with cells of radius 5 km, centered at those points with the coordinate vectors of (0,0) km, (8.66,0) km, (4.33,7.50) km, (-4.33,7.50) km, ..., and so on, which is depicted in the upper left corner of Fig. 5.

In the first simulation, we fix the MS location at (3,3) km and determine how the estimation errors of various algorithms are affected by the standard deviation (STD) of the range measurement errors. For convenience, we assume the range measurement errors for different BS-MS pairs to be identically distributed in the simulation. The simulation result is shown in Fig. 5, where the average location estimation errors versus standard deviations of the range measurement errors are compared. The comparison is made among the G-LS algorithm, the G-TS-LS algorithm, the LS solution accuracy, the W-TS-LS algorithm, the W-TS-LS-EI algorithm, the ML solution accuracy, and the proposed algorithm, where the only difference between the W-TS-LS algorithm and the W-TS-LS-EI algorithm is their initial guess. The W-TS-LS-EI algorithm uses the exact mobile location as its initial guess. However, the noisy initial guess used in the W-TS-LS algorithm is the same as that used in the proposed algorithm which is described in Section 3.3. The average error is evaluated over 10,000 independent trials. As expected, 1) the average location error increases when the STD of the range measurement error increases, 2) the average location errors of the conventional G-LS and the conventional G-TS-LS are lower bounded by the LS solution accuracy, 3) the average location errors of the proposed algorithm are not lower bounded by the LS solution accuracy, but by the ML solution accuracy, and 4) the proposed algorithm is superior to the G-LS algorithm, the G-TS-LS algorithm, the W-TS-LS algorithm, and the LS solution accuracy.

TABLE II

PROBABILITY THAT EACH OF VARIOUS POSITION LOCATION ALGORITHMS, WITH DIFFERENT RANGE MEASUREMENT ERROR STDS, MEETS THE 100 M FCC REQUIREMENT.

STD	Probability(error<100m)					
(m)	G-LS	G-TS-LS	LS	W-TS-LS	Proposed	ML
25	100%	100%	100%	99.84%	100%	100%
50	97.98%	98.18%	98.14%	98.51%	99.39%	99.40%
75	81.79%	83.18%	83.18%	92.86%	93.63%	93.97%
100	61.61%	63.36%	62.80%	84.10%	84.91%	85.99%
125	45.67%	47.15%	46.83%	73.15%	75.37%	77.05%
150	34.35%	35.84%	36.18%	62.79%	66.91%	69.31%
175	26.14%	26.93%	26.85%	53.49%	58.42%	63.00%
200	21.27%	21.87%	22.31%	46.50%	51.95%	56.58%

TABLE III

PROBABILITY THAT EACH OF VARIOUS POSITION LOCATION ALGORITHMS, WITH DIFFERENT RANGE MEASUREMENT ERROR STDS, MEETS THE 300 M FCC REQUIREMENT.

STD	Probability(error<300m)					
(m)	G-LS	G-TS-LS	LS	W-TS-LS	Proposed	ML
25	100%	100%	100%	100%	100%	100%
50	100%	100%	100%	99.99%	100%	100%
75	100%	100%	100%	99.91%	99.99%	99.99%
100	99.98%	99.98%	99.98%	99.70%	99.96%	99.96%
125	99.65%	99.70%	99.58%	99.45%	99.89%	99.89%
150	97.85%	98.17%	98.15%	98.64%	99.13%	99.14%
175	93.54%	94.43%	94.93%	97.23%	97.07%	98.20%
200	87.96%	89.12%	89.65%	95.52%	94.56%	95.99%

As mentioned in Section 1, the US FCC requires the cellular phone service providers to obtain the location information of an MS with such accuracy as to allow only 100 meters of maximum error tolerance for 67 percent of scenarios and 300 meters of that for 95 percent of scenarios in a network-side PL system. With different standard deviations (STDs) of the range measurement error, σ_{d_i}, Table II and Table III list the probabilities that the location errors of various PL algorithms are less than 100 meters and 300, respectively, based on 10,000 independent trials. Note that the upper right hand side of each table meets the FCC requirement, while the lower left hand side fails. It is observed that: 1) the proposed factor-graph-based algorithm always performs slightly worse than the optimum ML solution accuracy but much better than all the other algorithms; 2) when the range measurement error STD is greater than 125 m, no conventional algorithms can meet the FCC requirement; 3) when the range measurement error STD is larger than 150 m, no algorithms can meet the FCC requirement, not even the optimum ML solution.

Next, let us compare the PL algorithms in their performance dependence on the MS location. The average location errors as a function of the MS location is evaluated through computer simulation. In this simulation, the test region is the shadowed zone shown in the upper left corner of Fig. 5 and the involved BSs are *BS 1*, *BS 2*, *BS 3*, and *BS 4*. The results are illustrated in Fig. 6, where the x and y axes are the location coordinates

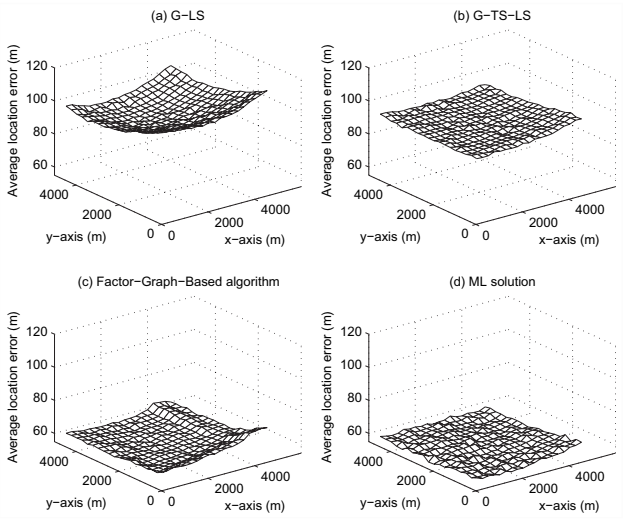

Fig. 6. Average location error versus MS location for (a) G-LS (b) G-TS-LS (c) proposed factor-graph-based algorithm (d) ML solution accuracy. Four BSs are assumed. The range measurement error is Gaussian distributed with standard deviation of 100 meters.

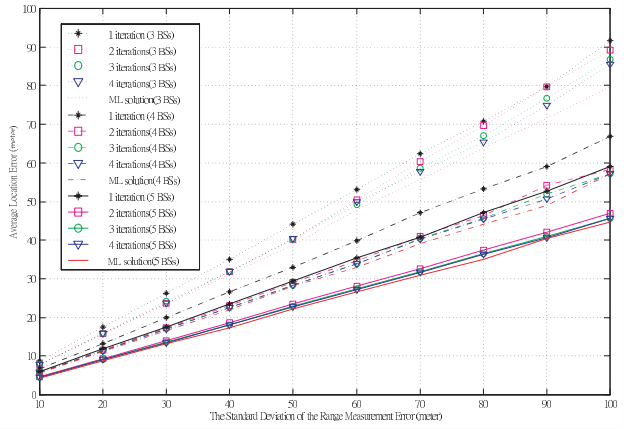

Fig. 7. Performance of the proposed algorithm with different number of BSs and with different number of iterations.

of the target MS. Simulation results show that the proposed algorithm outperforms the G-LS algorithm and the G-TS-LS algorithm. Moreover, among these algorithms, the proposed algorithm generally is the least sensitive to the MS location.

Let us consider the issue of system complexity. Both the ML solution and the LS solution have very high computational complexity, since they need to solve a system of non-linear equations. The most popular method for solving non-linear equations is the Newton's method [16]. On the other hand, the proposed algorithm needs only simple operations at each node to calculate the soft-information, i.e., mean and variance of the Gaussian pdf's, to be passed around. In addition, the computational complexity of the proposed algorithm is *linearly* proportional to N, while the number of the required derivatives alone in the Newton's method above is proportional to $(2N)^2$.

Finally, regarding the convergence issue of the proposed algorithm, Fig. 7 shows the iterative performance of the proposed algorithm with the number of the involved BSs ranging from three to five. We can see that the performance

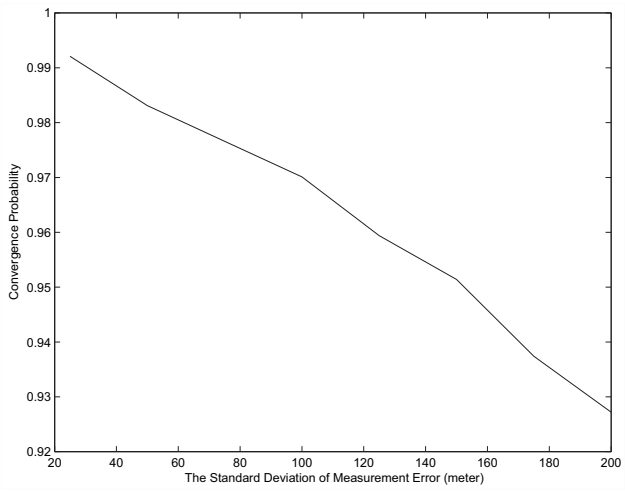

Fig. 8. Convergence probability of the proposed algorithm when the range measurement noise standard deviation ranging from 25 to 200 meters.

of the proposed algorithm approaches the ML solution accuracy after 4 iterations, which shows that the convergence speed of the proposed algorithm is reasonably high. On the other hand, we also test the convergence probability of the proposed algorithm in Fig. 8. Since the pdf of the TOA/range measurement noise extend all the way to infinity, no algorithm can always guarantee a reasonable solution in practice. From the simulation result, we find the proposed algorithm has a very high convergence probability. Even when the range measurement noise STD is 200 meters, the convergence rate of the proposed algorithm is still 92.62%.

VI. Conclusions

A new geolocation algorithm based on the TOA/range measurements is proposed to estimate the target MS location. The proposed algorithm efficiently utilizes the stochastic properties of measurement data by exchanging soft-information among local processing units in a factor graph. Because of the distributed feature of the proposed algorithm, one may suspect the proposed algorithm to sometimes degrade the PL accuracy. Fortunately, simulation results show that the PL mean square error gap between the ML solution accuracy and the proposed algorithm is quite small. In addition, the proposed algorithm enjoys low computational complexity and its distributed feature makes it quite suitable for integrated-circuit implementation.

References

[1] Y. Zhao, "Standardization of mobile phone positioning for 3G systems," *IEEE Commun. Mag.*, vol. 40, no. 7, pp. 108-116, July 2002.
[2] Q. Bi, G. L. Zysman, and H. Menkes, "Wireless mobile communications at the start of the 21st century," *IEEE Commun. Mag.*, vol. 39, no. 1, pp. 110-116, Jan. 2001.
[3] J. Caffery, Jr. and G. Stuber, "Overview of wireless location in CDMA systems," *IEEE Commun. Mag.*, vol. 36, no. 4, pp. 38-45, Apr. 1998.
[4] J. Caffery, *Wireless Location in CDMA Cellular Radio Systems*. Kluwer Academic Publishers, 1999.
[5] J. Caffery, Jr. and G. Stuber, "Subscriber location in CDMA cellular networks," *IEEE Trans. Veh. Technol.*, vol. 47, pp. 406-416, May 1998.
[6] M. Hata and T. Nagatsu, "Mobile location using signal strength measurements in a cellular system," *IEEE Trans. Veh. Technol.*, vol. 29, pp. 245-251, May 1980.
[7] M. I. Silventoinen and T. Rantalainen, "Mobile station emergency locating in GSM," in *Proc. IEEE International Conference on Personal Wireless Communications*, pp. 232-238, 1996.
[8] J. Caffery, "A new approach to the geometry of TOA location," in *Proc. IEEE Vehicular Technology Conference,* vol. 4, pp. 1943-1949, Sept. 2000.
[9] W. H. Foy, "Position location solutions by Taylor-Series estimation," *IEEE Trans. Aerosp. Electron. Syst.*, vol. 12, no. 2, pp. 187-193, Mar. 1976.
[10] J-C. Chen, C-S. Maa, Y-C. Wang, and J-T. Chen, "Mobile position location using factor graphs," *IEEE Commun. Lett.,* vol. 7, pp. 431-433, Sept. 2003
[11] F. R. Kschischang, B. J. Frey, and H.-A. Loeliger, "Factor graphs and the sum-product algorithm," *IEEE Trans. Inform. Theory*, vol. 47, pp. 498-519, Feb. 2001.
[12] M. P. Wylie and J. Holtzman, "The non-line of sight problem in mobile location estimation," in *Proc. IEEE International Conference on Universal Personal Communications*, pp. 827-831, 1996.
[13] L. Cong and W. Zhang, "Hybrid TDOA/AOA mobile user location for wideband CDMA cellular systems," *IEEE Trans. Wireless Commun.*, vol. 1, pp. 439-447, July 2002.
[14] D. J. Torrieri, "Statistical theory of passive location systems," *IEEE Trans. Aerosp. Electron. Syst.*, vol. 20, no. 2, pp. 183-198, Mar.1984.
[15] Y. Qi and H. Kobayashi, "A unified analysis for Cramer-Rao lower bound for geolocation," in *Proc. 36th Annual Conference on Information Sciences and Systems*, Mar. 2002.
[16] G. Lindfield and J. Penny, *Numerical Methods Using MATLAB*. Ellis Horwood Limitd, 1995.

Jung-Chieh Chen received the B.S. degree in electrical engineering from the Tatung Institute of Technology, Taipei, Taiwan, R.O.C., the M.S. degree in electrical engineering from the National Chung Cheng University, Chiayi, Taiwan, and the Ph.D. degree in communications engineering from the National Tsing Hua University, Hsinchu, Taiwan. Since August 2005, he has been a faculty member at National Kaohsiung Normal University, Kaohsiung, Taiwan. His research interests include wireless communication systems, radio resource management, radio location techniques, and graphical approach for information processing.

Yeong-Cheng Wang received the B.S.C.E. and M.S.E.E. degrees from the National Taiwan University, Taipei, Taiwan, R.O.C., in 1984, and 1989, respectively, and Ph.D. degree in electrical engineering from the University of Florida in 1994. Since August 1997, he has been a faculty member at VaNung University, Chung-Li, Taiwan. His current activities is in system integration of wireless communication systems.

Ching-Shyang Maa was born in Tainan, Taiwan, R.O.C., in 1976. He received the B.S., M.S., and Ph.D. degrees from the National Tsing Hua University, Hsinchu, Taiwan, R.O.C., in 1998, 2000, and 2004, respectively, all in electrical engineering. Since October 2004, he has been with Genesys Logic, Inc., Taipei, Taiwan, R.O.C., where he works on the design and implementation of OFDM-related systems. His current research interests include wireless communications, MIMO OFDM systems, and space-time coding.

Jiunn-Tsair Chen received his BS degree from National Chiao-Tung University in 1986, received his MS degree from National Taiwan University in 1989, received his Ph.D from Stanford University in 1998, all in electrical engineering. Since August, 1999, he joined National Tsing Hua University, Hsinchu, where he is currently working as an associate professor. His research interests include wireless communications, antenna array signal processing, adaptive digital signal processing, and power amplifier linearization.